MicroDERLab

University Politehnica of Bucharest

Title: Online optimization of a multi-conversion-level DC home microgrid for system efficiency enhancement

Authors: V. Boscaino, J.M. Guerrero, I. Ciornei, L. Meng, E. Riva Sanseverino and G. Zizzo

Published in: Elsevier Journal - Sustainable Cities and Society

DOI (link to publication from Publisher): https://doi.org/10.1016/j.scs.2017.08.014

Publication date: 11/2017

Citation for published version:
V. Boscaino, J. M. Guerrero, **I. Ciornei**, L. Meng, E. Riva Sanseverino, and G. Zizzo, "Online optimization of a multi-conversion-level DC home microgrid for system efficiency enhancement," *Sustain. Cities Soc.*, vol. 35, pp. 417–429, Nov. 2017.

Acknowledgement: This work has received funding from the European Union's Horizon 2020 R&I Programme under the Marie Sklodowska-Curie grant agreement No 708844

Sustainable Cities and Society 35 (2017) 417–429

Contents lists available at ScienceDirect

Sustainable Cities and Society

journal homepage: www.elsevier.com/locate/scs

Online optimization of a multi-conversion-level DC home microgrid for system efficiency enhancement

V. Boscaino[a], J.M. Guerrero[b], I. Ciornei[c], L. Meng[b], E. Riva Sanseverino[a], G. Zizzo[a,*]

[a] Department of Energy, Information Engineering and Mathematical Models, Università di Palermo, Palermo, Italy
[b] Department of Energy Technology, Aalborg University, Aalborg, Denmark
[c] Polytechnic University of Bucharest, Bucharest, Romania

ARTICLE INFO

Keywords:
DC microgrids
Active droop control
Current sharing
Genetic algorithm
Master-slave control
Power conversion efficiency
Peak shaving

ABSTRACT

In this paper, an on-line management system for the optimal efficiency operation of a multi-bus DC home distribution system is proposed. The operation of the system is discussed with reference to a distribution system with two conversion stages and three voltage levels. In each of the conversion stages, three paralleled DC/DC converters are implemented. A Genetic Algorithm performs the on-line optimization of the DC network's global efficiency, generating the optimal current sharing ratios of the concurrent power converters. The overall DC/DC conversion system including the optimization section is modelled using MATLAB/Simulink. Thanks to the implemented online algorithm, considering the system modelling as dynamic master/slave configuration, reliability, robustness and flexibility of the whole conversion system is enhanced. Since an online algorithm is implemented, several variables are accounted for, such as: components loss parameters, components ageing, load currents, switching frequency and input voltage. Simulation results considering several case studies are presented and the benefits brought by the optimization algorithm in terms of power saving are widely discussed for each case study.

1. Introduction

Nowadays, many Direct Current (DC) devices are available only for very low voltage levels (from 5 V to 48 V) and for automation and telecommunication applications. Nevertheless, thanks to the possibility of achieving significant energy savings (Amin, Arafat, Lundberg, & Mangold, 2011a), there are also many example of applications of higher DC voltages (up to 1500 V) in some specific fields like data centres and ICT but also in the industrial sector (Kakigano, Miura, Ise, Van Roy, & Driesen, 2012; Nilsson & Sannino, 2004; Nuutinen et al., 2014; Rekola & Tuusa, 2014).

ICT equipment, lighting, consumer electronics, portable white goods, all utilize DC voltage (Garbesi, Vossos, & Shen, 2011; Yoza, Uchida, Yona, & Senjyu, 2012). DC distribution offers to renewable energy-based generators and battery storage systems, an easier and more efficient integration in modern smart grid as compared to Alternative Current (AC) solutions. Together with the ever increasing shares of renewable energy sources, more and more DC supplied electronic appliances and DC compatible appliances are shifting worldwide distribution networks towards DC.

The advantage over AC seems to be increasing as the effects of topology and components developments on Low Voltage DC (LVDC) energy efficiency are accounted for (Lana et al., 2015).

These elements are able to induce a rapid increase of interest in the use of DC systems in residential, commercial and industrial applications (Laudani & Mitcheson) and to drive the evolution of future electrical distribution systems towards the use of DC architectures and components (Diaz, Vasquez Quintero, & Guerrero, 2016).

Practical examples supporting this trend can already be seen worldwide: in Japan, US, Korea and EU Countries.

Due to the potential benefits they may bring in terms of energy savings and reduction of a number of inherent problems to AC power distribution, researchers and manufactures are focusing part of the research efforts also through the implementation of prototype installations of DC microgrids. Japan is currently the most advanced country in DC systems implementation, with a special focus on residential applications. Two main DC test systems were built in Island City in Fukuoka City and in Tohoku Fukusi University in Sendai City. The main reason of its success is the need to create resilient solutions after the tsunami in 2011. Still in Asia, in Taiwan, a demonstration grid connected DC facility including different energy resources has been built recently (Wu, Chen, Yu, & Chang, 2011).

* Corresponding author.
E-mail address: gaetano.zizzo@unipa.it (G. Zizzo).

http://dx.doi.org/10.1016/j.scs.2017.08.014
Received 11 May 2017; Received in revised form 21 July 2017; Accepted 8 August 2017
Available online 25 August 2017

Nomenclature

AC	Alternative current
D_j	Duty-cycle of the *j*-th second level converter
DC	Direct current
d(s)	Laplace transform of the duty cycle function
GA	Genetic algorithm
HEV	Hybrid electric vehicles
ICT	Information and communication technology
$i_L(s)$	Laplace transform of the inductor current
I_{in2}	Total amount of the second DC level input current
I_{2Lj}	Inductor current of the *j*-th second level converter
IoT	Internet of things
$I_{tot,1}$	Load current of the first DC level
$I_{tot,2}$	Load curren of the second DC level
LUT	LookUp table
LV	Low voltage
LVDC	Low voltage direct current
p_{cross}	Crossover probability
p_{mut}	Mutation probability
Pl(i,j)	Power losses of the j-th concurrent converter on the i-th level
Po(i,j)	Output power of each j-th concurrent converter on the i-th level
PS	Peak shaving
η_{ij}	Efficiency value of the j-th converter within the i-th level.
R_{dij}	Virtual resistance of the j-th converter in the i-th conversion level
R_{L2}	Load resistance of the second level of conversion
$_{L1}$	Load resistance of the first level of conversion
I_{in2}	Input current of the second conversion level
V_{dcij}	Reference value of the DC output voltage of the j-th converter in the i-th level
V_{dc2}	Output voltage of the first conversion level
V_{dc3}	Output voltage of the second conversion level
V_{refi}	Rated value of the DC output voltage of the i-th level

In Europe, Aalborg University hosts the DC Home laboratory, based on a three level multi-bus architecture (24 V/48 V/380 V) and still under development, aiming to demonstrate the viability of technical and cost advantages of using LVDC technology for supplying residential consumers in place of traditional AC systems (Anonymous, 2017; Diaz et al., 2015).

Other examples of DC microgrid systems can be found in (Justo, Mwasilu, Lee, & Jung, 2013). Among these, one of the most advanced is the Sweden UPN AB for Data center IBM, based on a 24 V/280 V LVDC distribution. As far as experimental setups are concerned, the work in (Kakigano, Miura, Ise, Momose, & Hayakawa, 2008) presents a 100 V DC microgrid test system with a gas engine cogeneration machine, while the work in (Sasidharan, Madhu M., Singh, & Ongsakul, 2015) characterizes and implements an efficient hybrid AC/DC solar powered home grid system.

Other papers simulate DC distribution. As an example, in (Sasidharan & Singh, 2017; Sasidharana, Madhu Ma, Govind Singha, & Ongsakul, 2015) a community of 100 hybrid AC/DC houses with photovoltaic and wind system and real time grid ancillary services provision is studied.

From what emerges from the literature, if compared with their AC counterparts, DC distribution networks are generally less affected by frequency synchronization requirements and power quality related issues (Madduri et al., 2015; Dragicevic, Vasquez, Guerrero, & Skrlec, 2014; Dragĭcevíc, Lu, Vasquez, & Guerrero, 2016, 2016b). Higher efficiency, great flexibility and reduced capital cost can be achieved. If natively DC loads are addressed, benefits brought by DC distribution are heightened (Glasgo, Azevedoa, & Hendricksonb, 2016; Vossos, Garbesi, & Shen, 2014), under very specific assumptions concerning end use, and kind of intervention. Yet, the efficiency optimization is a key issue to be addressed (Rodriguez-Diaz, Vasquez, & Guerrero, 2016).

At the same time, the growing presence and use of smart devices and energy efficient appliances reveals a promising future for smart DC houses integrated in the Internet of Things (IoT), where residential electrical power systems work in cooperation to achieve smarter, more sustainable, and cleaner energy systems (Glasgo et al., 2016; Rodriguez-Diaz et al., 2016; Vossos et al., 2014; Weixing, Xiaoming Mo, Yuebin, & Marnay, 2012a).

Even if research is moving towards a 48 V home utility, voltage levels are not yet standardized and actually designed on the basis of the load power appliances consumption (Amin, Arafat, Lundberg, & Mangold, 2011b; Makarabbi, Gavade, Panguloori, & Mishra, 2014).

In this context, it is fundamental to design more and more efficient and reliable DC/DC converter topologies and architectures for supplying DC appliances connected to DC microgrids

In the present work, the design of an optimal energy management system for load sharing within a single DC residential unit is addressed. The main contribution of this work is the definition of a heuristic-based on-line global optimization algorithm that maximizes the overall efficiency of the DC/DC conversion system, based on an unbalanced current sharing among concurrent converters. Heuristic optimization, in particular a standard Genetic Algorithm (GA) (Goldberg, 1989), is chosen due to the non-linear nature of the objective function related to efficiency, and of the constraints. For the calculations, the GA solver available in MATLAB has been employed.

In the literature, the most common solution for multi-bus approaches includes several parallel converters for each conversion level in order to enhance the conversion efficiency of the whole system. A balanced load sharing among concurrent converters (Nasirian, Davoudi, & Lewis, 2014; Guerrero, Vasquez, Matas, de Vicuna, & Castilla, 2011) is thus needed and typically, the efficiency optimization is commonly based on a simple master-slave configuration. Under light load conditions, only the master module is active while, at heavy load all modules are active and slave units are progressively activated by the master unit according to the instantaneous load power demand.[1] Load current thresholds for the progressive activation of each slave unit are fixed. On-line algorithms can provide a further efficiency enhancement based on an on-line adjustment of the current sharing ratios according to the instantaneous load current demand.

The proposed optimization algorithm is applied to a 24 V/120 V/325 V DC distribution network that is supposed supplying a house, including primary and secondary controllers. The choice of the voltage levels is not strictly meaningful, since the focus of the paper is on the methodology and on the proof of concept of the adaptive on-line optimizer for the considered topology, as compared to standard energy management implementations for concurrent DC/DC converters. The system under examination comprises only DC loads but could comprise also DC/AC converters for supplying specific energy intensive loads that currently can't be supplied by a DC network (for example some white goods).

With respect to a previous study where the system behavior of such a system was examined only with reference to load transients (Riva Sanseverino, Zizzo, Boscaino, Guerrero, & Meng, 2017), the

[1] Light load and heavy load are defined with reference to the load current which the efficiency peak corresponds to. Light load or low current region comprises all the load conditions characterized by a value of the load current below the efficiency peak current. Heavy load or high current region comprises all the load conditions characterized by a value of the load current higher than the efficiency peak current.

performance of the optimization algorithm is here tested in various conditions. Simulation results show that the overall system efficiency is enhanced by using the proposed control architecture with respect to the traditional one also in presence of Demand Response policies based on Peak Shaving (PS).

2. Proposed DC home architecture

The architecture of the Low Voltage distribution is a multi-bus three levels (24 V/120 V/325 V) DC system (Fig. 1). Besides for the aims of this paper it is not important, the choice of the three levels is justified as it follows.

The 24 V bus is dedicated to the supplied of low power peak DC appliances among which lamps, fans and doorphones, can be cited as examples.

A 120 V intermediate bus is then considered. Even if research is moving towards a standardized 48 V voltage level (Das, Fatema, & Anower, 2016), in the literature several comparative studies show that a 120 V voltage level is the highest DC value allowing losses saving (Weixing, Xiaoming Mo, Yuebin, & Marnay, 2012b). Moreover, 120 V DC is the limit for extra-low voltage systems and thus it assures a proper safety against electric shock in DC microgrids (IEC Standard, 2005). Therefore, in the proposed configuration the 120 V DC level is used for supplying high and medium power peak DC appliances like dishwashers, washing machines, air-conditioners, etc. guarantying safety for persons and, at the same time, reducing the current circulating on the cables and the consequent energy losses.

Finally, the 325 V DC voltage produces on cable insulation the same stress of the standard 230 V AC level, and therefore is fully compatible with the existing building cabling. In our study, we have considered no loads supplied with this voltage level, being higher than the extra-low voltage limit. Nevertheless, the possibility to have a higher voltage level at the house premises, allows a more efficient connection of local DC generators (photovoltaic or wind generators) and the reduction of voltage drops and power losses in the main distribution especially in large buildings. Indeed, in large buildings, internal distribution lines can also reach 100 m or even more, thus producing high voltage drops and power losses if operated at very low voltages and requiring costly copper wirings.

The DC conversion network model is implemented using MATLAB/Simulink. As shown in Fig. 1, for each conversion stage three DC/DC buck converters are considered.

3. Power conversion systems

As already said, the system architecture is conceived with two levels of conversion: 325 V–120 V and 120 V–24 V. Fig. 2 shows the architecture of the i-th level of conversion (the system architecture is the same for both levels). Each level includes three step-down paralleled buck converters (*Converter,ij*), modelled by the small signal equations. Fig. 2 shows a local controller for each converter and one secondary controller. The local controllers implement droop control and inductor current control while the secondary controller implements voltage restoring (Dragičević et al., 2016a, 2016b).

The first-level and second-level output voltages are referred to as V_{dc2} and V_{dc3}, respectively.

The second level load current is derived from the loads directly connected to the second level output:

$$I_{tot,2} = \frac{V_{dc3}}{R_{L2}} \tag{1}$$

where R_{L2} is the equivalent resistance of the overall load of the second level.

The two levels of conversion are cascaded, therefore, the first-level load current is obtained as:

$$I_{tot,1} = \frac{V_{dc2}}{R_{L1}} + I_{in2} \tag{2}$$

where R_{L1} is the equivalent resistance of the overall load of the first level and I_{in2} is the total amount of the second-level input current.

The input current of each second-level power converter is derived by the step-down buck converter input-output current relationship:

$$I_{in2} = \sum_{j=1}^{3} I_{2Lj} \cdot D_j \tag{3}$$

where I_{2Lj} is the inductor current and D_j the duty-cycle of the *j*-th second level converter.

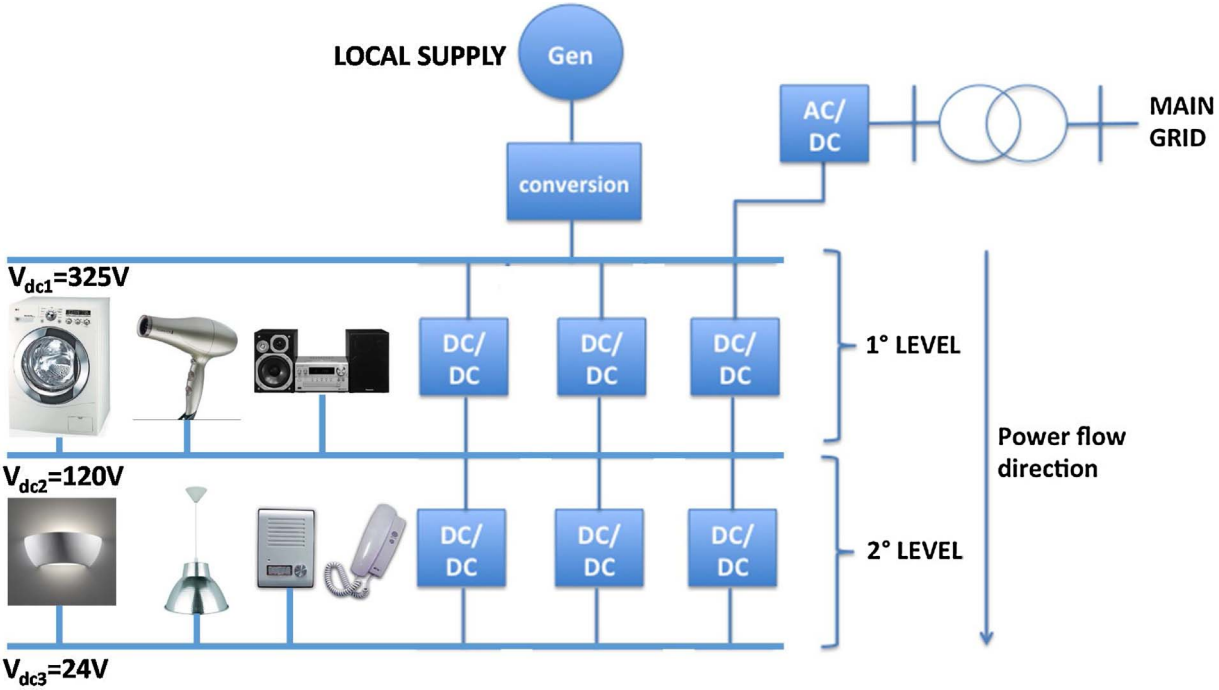

Fig. 1. Multibus DC system architecture.

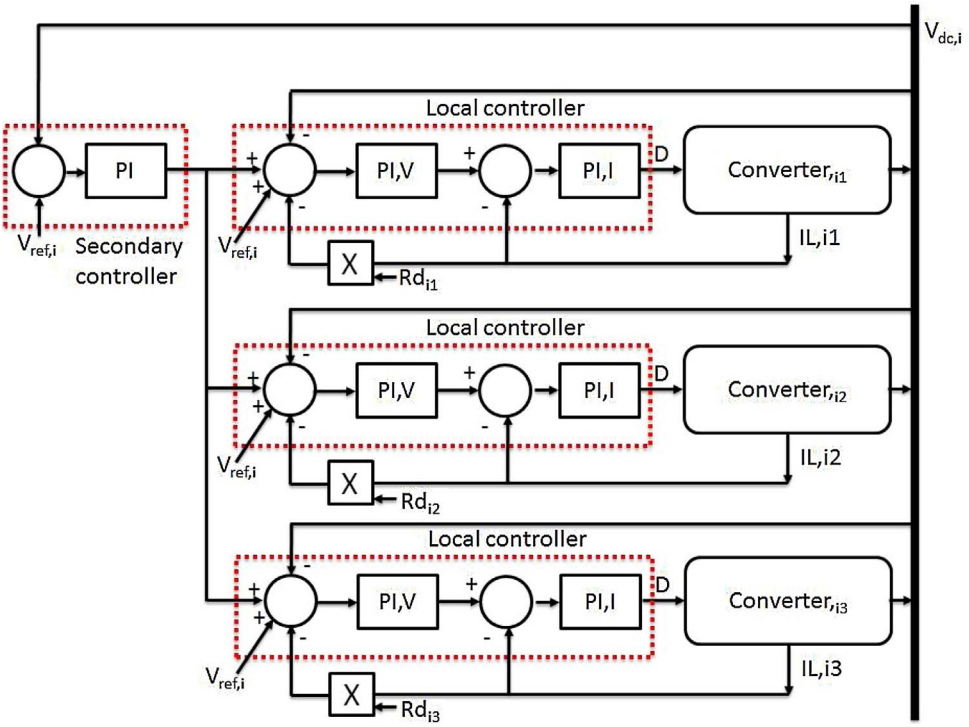

Fig. 2. Architecture of the i-th conversion level.

The online efficiency optimization technique applied in this paper is based on an unequal current sharing among the concurrent power converters. Figs. 3 and 4 show the efficiency curves as a function of the load current of each first-level and second-level converter, respectively. The curves are obtained experimentally at the Aalborg laboratory, according to the procedure described in (Klimczak & Munk-Nielsen, 2008).

The efficiency optimization algorithm is conceived to find the optimal current sharing ratios to maximize the power conversion efficiency of the whole power system. If equal droop resistances are fixed, equal current sharing will be achieved for concurrent converters.

The optimal current sharing ratios are selected to minimize system power losses by means of an online GA (Goldberg, 1989), implemented by a MATLAB script and properly integrated within the Simulink schematic of the DC distribution network. The use of heuristics instead of classical deterministic optimization is advisable due to the highly non linear nature of efficiency curves of DC converters. Online algorithm are preferred to off-line algorithms because the efficiency depends on several variables among which the switching frequency, the loading currents, the input voltage, components' ageing and components' loss parameters.

An adaptive LookUp Table (LUT) is implemented to store experimental efficiency data set for each power converter. A proper power load current sequence is forced to make the adaptive LUT to learn the efficiency curves coming from the experimental data set. The system is thus conceived to emulate the experimental setup. The conversion level is loaded by a specific load current sequence, the efficiency values of each concurrent power converter are measured and stored in a LUT to be used for the optimization problem.

The effects of input voltage and switching frequency on the efficiency curves are reasonably neglected because each conversion subsystem is fed by a regulated DC bus and a constant switching frequency control is applied. The online algorithm is implemented to minimize the objective function OF of each conversion level, as given by:

$$OF = sum[OF_i] = \sum_{j=1}^{3} Pl(i,j) \tag{4}$$

$$Pl(i,j) = Po(i,j)\left(\frac{1-\eta_{ij}}{\eta_{ij}}\right) \tag{5}$$

Z

where Pl(i,j) indicates the power losses of each j-th concurrent converter on the i-th level expressed as a function of the output power Po (i,j) and of the efficiency value ηij of the j-th converter within the i-th level.

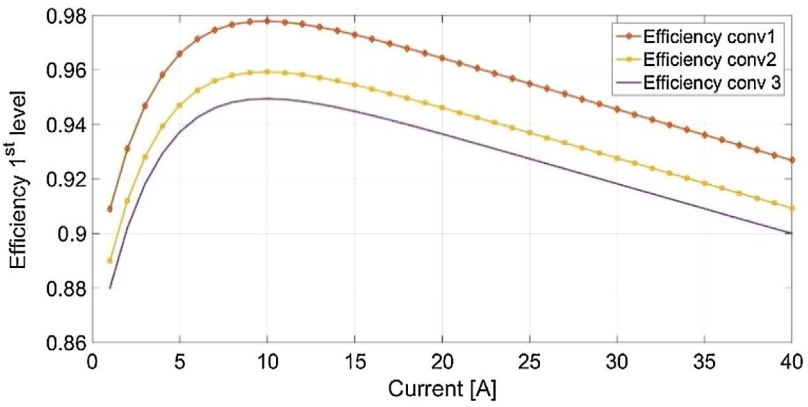

Fig. 3. Experimental data set of efficiency of each concurrent converter of the first level of conversion.

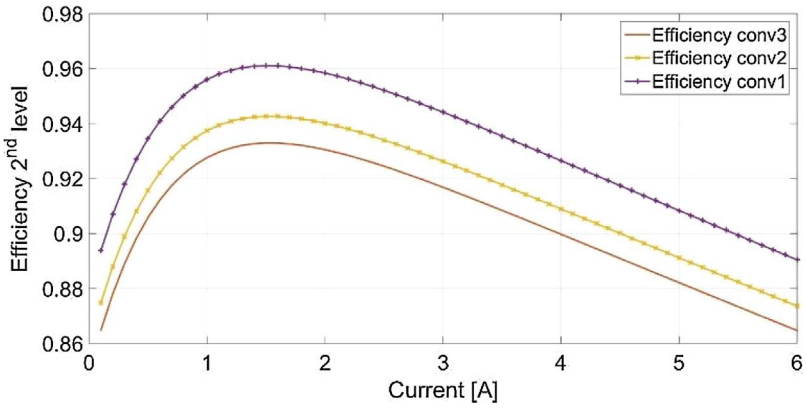

Fig. 4. Experimental data set of efficiency of each concurrent converter of the second level of conversion.

For minimizing the objective function OF, the GA generates the optimal operating current values of each concurrent converter subjected to the following costraints:

$$\begin{cases} \sum_{j=1}^{3} i(i,j) = I_{tot,i} \\ i(i,j) \le I_{tot,i}\ j = 1, 2, 3 \\ i(i,j) \ge 0\ j = 1, 2, 3 \end{cases} \quad (6)$$

For each conversion level, the total load current of the corresponding DC output bus and the efficiency data set of each converter are the algorithm input data.

In order to adjust the output current of each concurrent converter, the online algorithm is interfaced with the active droop control integrated in the local controller of each conversion level. The droop control acts as a virtual resistance R_{dij} on the voltage loop control, that affect the load sharing among concurrent power converters of the i-th level and thus the currents injected by each one to the voltage bus:

$$V_{dcij} = V_{refi} - R_{dij} I_{ij} \quad (7)$$

In (7), V_{dcij} and V_{ref} are the reference value of the DC output voltage of the j-th converter and the rated value of the DC output voltage, respectively, and i_{ij} and R_{dij} are the output current and virtual resistance of the j-th converter in the i-th level, respectively.

Optimal virtual resistances are derived from the optimal converter current values, according to:

$$i(i,1): i(i,2): i(i,3) = \frac{1}{R_{di1}}: \frac{1}{R_{di2}}: \frac{1}{R_{di3}} \quad (8)$$

Values of virtual resistances are forced within the range of system stability 0.1 Ω/2 Ω and 0.01 Ω/0.5 Ω for the 1 st and 2nd levels, respectively. The GA algorithm outputs the optimal current values for each concurrent converter and optimal droop parameters of the i-th level are obtained by optimal current values according to (8). Tables 1 and 2 synthetizes the general optimization problem and the GA parameters.

Fig. 5 shows the architecture of the optimization subsystem for one level of conversion. A MATLAB script implementing the GA algorithm is included in the Optimization GA algorithm subsystem. R_{d1}, R_{d2},R_{d3} are the virtual resistances applied to the level of conversion within each local controller after each GA execution. The inputs of the GA algorithm are the total output current of the level of conversion i_{total} and the LUTs' efficiency values, after the learning process. The clock signal is used to enable the GA after the learning process of implemented LUTs.

Table 2
Genetic Algorithm parameters.

Optimization algorithm	Coding	Population size	Termination condition	Mutation and crossover probability
Real coded Genetic Algorithm	Real	40	(Number of iterations: 200) or (Flattening of improvement of OF < 1e-4)	p_{mut} = 0.1 p_{cross} = 0.7

In order to maximize the power conversion efficiency of the whole conversion system, optimal current sharing ratios are determined by the GA algorithm leading to a dynamic master-slave configuration.

Considering that the efficiency of three paralleled converters can be obtained as:

$$\eta_{level}(i) = \frac{Pout_{level}}{Pin_{level}} = \frac{Pout_{level}}{\frac{P_{o1}}{\eta_1(i')} + \frac{P_{o2}}{\eta_2(i'')} + \frac{P_{o3}}{\eta_3(i''')}} = \frac{1}{\frac{P_{o1}/Pout_{level}}{\eta_1(i')} + \frac{P_{o2}/Pout_{level}}{\eta_1(i'')} + \frac{P_{o3}/Pout_{level}}{\eta_3(i''')}} \quad (9)$$

the GA algorithm optimizes current ratios to maximize the power conversion efficiency. The converter featuring the highest actual efficiency carries out the most of the load current. For very light load (namely small load currents) conditions, the converter featuring the highest efficiency carries out all of the load current. The highest efficiency converter behaves as the master converter and the others behave as slave converters. Notwithstanding this, if a fault occurs on the master

Table 1
General optimization problem description.

Optimization variables	Optimization parameters	Constraints	Objective function
Rdi1, Rdi2, …. Inductor currents	Load currents	$i_{ini} + \text{sum}(i_{ij}) = I_{Li\ i\ =\ level;j\ =\ converteratleveli}$ $Rd_{i1}\ i_{i1} = Rd_{i2}\ i_{i2} = \ldots\ Rd_{i,nconv\_lev\_i}\ i_{i,nconv\_lev\_i}$	$\sum_{i=1}^{nlevels} OFi = \sum_{i=1}^{nlevels} \sum_{j=1}^{nconv.lev.i} Pl(i,j)$ $Pl(i,j) = Po(i,j)\left(\frac{1-\eta_{ij}}{\eta_{ij}}\right)$

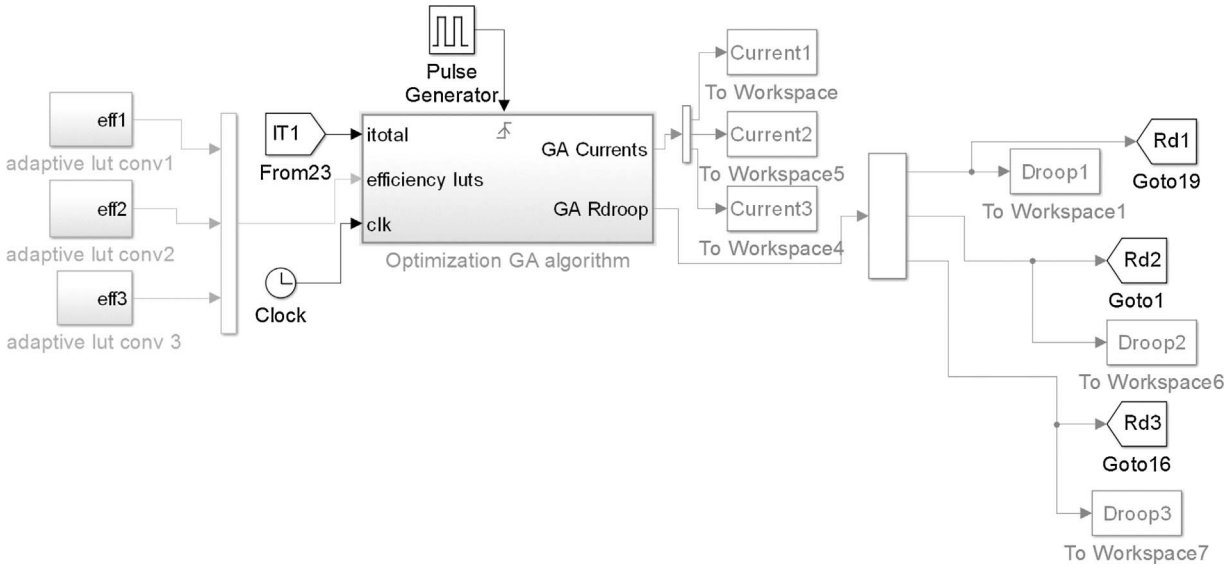

Fig. 5. Model of the optimization section.

converter, the GA algorithm receives a value of efficiency from the faulted converter equal to zero. Consequently, the online algorithm automatically runs with the remaining working converters appointing a new master converter to carry out the most of the current. Thanks to the online algorithm, a fault on the actual master converter will not lead to a fault of the whole power system. Therefore, the online algorithm enhances the reliability, robustness and flexibility of the power system.

4. Case studies

The proposed system is simulated under different scenarios to highlight the benefits brought by the GA. Firstly, load current step transients are considered, then, the system is tested under a real home daily power profile. In this second case, the DC home daily power profile is applied with and without GA and benefits brought by GA in terms of power saving are widely discussed. Finally, a peak shaving action is applied to the daily load profile further enhancing the power saving. Simulation results are presented and discussed to validate the proposed solution for LVDC microgrids.

4.1. GA optimization under load transient

The system is tested considering load power transients in both levels of conversion. Simulation starts under 1 A load current on the second level and no directly connected appliances to the first level. At 3 s a 5 A width load current step occurs at the second level. At 6 s a 40 A width load current step occurs at the first level. The GA is executed at a constant rate of 0.1 s.

Figs. 6 and 7 show the simulation results of the second and first level of conversion, respectively.

As shown in Fig. 6, initially, under light load conditions unequal current sharing occurs at the second level. The first converter, which is the highest efficiency converter, is the master converter and carries the whole load current, while the other converters carry no currents. At 3s, the load transient occurs. The second level of conversion moves towards heavy load condition of 6 A (higher loads). After the load transient, at the consecutive GA execution the current is almost balanced and finely adjusted among the concurrent converters in order to maximize the level efficiency. Slight unbalance under heavy load condition is due to

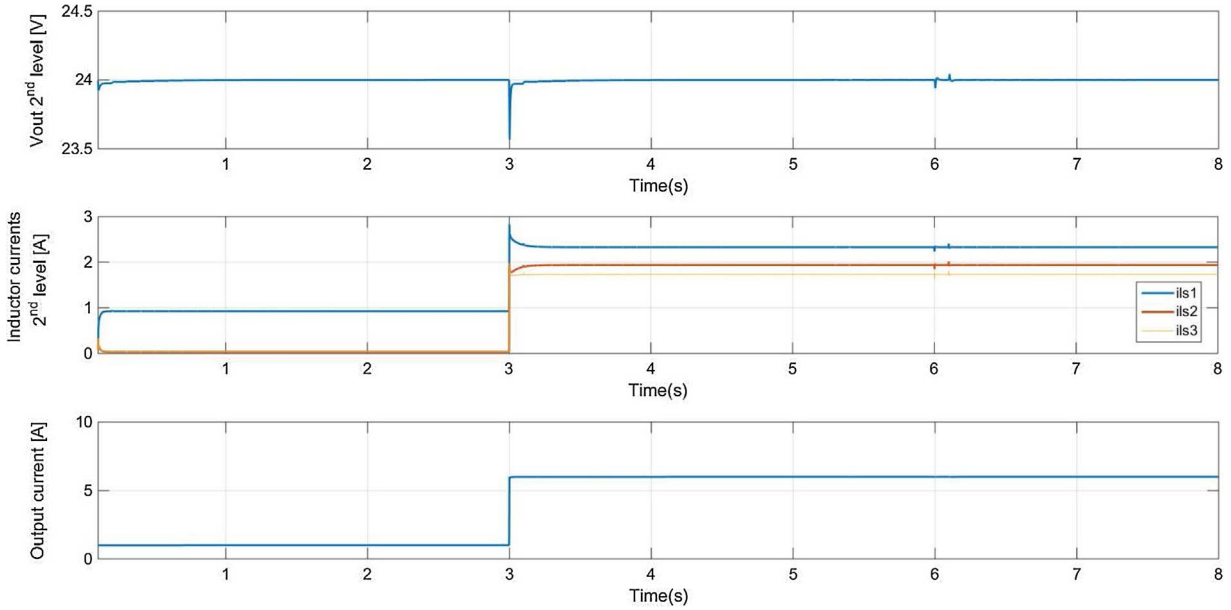

Fig. 6. Load current step on the second level of conversion.

differences in the efficiency curves of the power converters.

Similarly, in Fig. 7, the first level of conversion initially works under light load condition with the master converter carrying all of the load current. At 6 s a 40 A width load current step occurs at the first level of conversion. Firstly, the master converter is subjected to the most of load transient but, at the subsequent execution of the GA, the total load current is almost balanced among the three concurrent converters and the current ratios are finely adjusted around a balanced sharing condition. Actually, unequal current sharing is obtained because converters shows different efficiency curves. The current sharing ratio is the optimal ratio that minimizes the power losses of the whole DC conversion network.

4.2. Simulated efficiency curves

As already described, an adaptive LUT was implemented for each power converter to store efficiency values generated from the experimental data set. When the system starts, the GA is disabled for both conversion levels. A current learning sequence is forced at the output of each conversion level. The current is equally balanced among concurrent power converters. The corresponding efficiency of each converter is measured at each current value and the LUT is adapted storing experimental data set. For the first level of conversion, fourty equally distributed values in the range 1 A/40A are fixed as learning sequence. Sampling time of the learning sequence is fixed at 200 ms. Fig. 8 reports the initial random efficiency values stored in the adaptive LUT, and the final LUT values corresponding to the converter efficiency curve at the end of the learning process. The learning process lasts 8 s after which the GA is enabled.

Similarly, for the second level of conversion, twentyfive equally distributed current values are selected in the range 1 A/6 A. Fig. 9 shows the learning process for a single converter of the second level of conversion. Current values are sampled every 0.2 s and after 5 s the learning process is finished and the GA is enabled.

The system has been simulated under different load current conditions with and without GA. Fig. 10 compares the efficiency curves for the first level: the efficiency curve of each concurrent converter, the efficiency curve of the whole first level of conversion with GA and the efficiency curve of the whole first level of conversion without GA. Benefits brought by the GA implementation are highlighted in Fig. 10. Within the heavy load region, the load current is almost equally balanced among the concurrent converters and the curves nearly overlaps. At light load conditions (or low current conditions), the GA optimizes the current ratios to maximize the efficiency of the whole conversion system. In the light load region, the highest efficiency converter carries all the load current. In this condition, the GA efficiency curve and the converter efficiency curve overlaps. The efficiency curve without GA can be obtained considering equal current sharing among concurrent converters, as given by:

$$\eta_{1stlevel}(i) = \frac{Pout_{1stlevel}}{Pin_{1stlevel}} = \frac{Pout_{1stlevel}}{\frac{P_{o11}}{\eta_{11}\left(\frac{i}{3}\right)} + \frac{P_{o21}}{\eta_{21}\left(\frac{i}{3}\right)} + \frac{P_{o31}}{\eta_{31}\left(\frac{i}{3}\right)}} = \frac{1}{\frac{1}{3\eta_{11}\left(\frac{i}{3}\right)} + \frac{1}{3\eta_{21}\left(\frac{i}{3}\right)} + \frac{1}{3\eta_{31}\left(\frac{i}{3}\right)}} \quad (9)$$

where η_{j1} is the efficiency of the j-th converter of the first level of conversion and Po_{j1} is the output power of the j-th converter of the first level of conversion. The peak difference of efficiency of the whole first level is equal to 5.74% at 4 A load current.

Fig. 11 shows the comparison between the efficiency curves of each concurrent power converter of the second conversion level, the efficiency curve of the whole level with GA and the efficiency curve of the whole level without GA. Benefits brought by GA are highlighted by simulation results. The peak difference of efficiency of the whole second level of conversion with and without GA is equal to 5.19% at 0.8 A. The efficiency curve without GA can be obtained considering equal current sharing among concurrent converters, as given by:

$$\eta_{2ndlevel}(i) = \frac{Pout_{2ndlevel}}{Pin_{2ndlevel}} = \frac{Pout_{2ndlevel}}{\frac{P_{o12}}{\eta_{12}\left(\frac{i}{3}\right)} + \frac{P_{o22}}{\eta_{22}\left(\frac{i}{3}\right)} + \frac{P_{o32}}{\eta_{32}\left(\frac{i}{3}\right)}} = \frac{1}{\frac{1}{3\eta_{12}\left(\frac{i}{3}\right)} + \frac{1}{3\eta_{22}\left(\frac{i}{3}\right)} + \frac{1}{3\eta_{32}\left(\frac{i}{3}\right)}} \quad (10)$$

where η_{j2} is the efficiency of the j-th converter of the second level of conversion and P_{oj2} is the output power of the j-th converter of the second level of conversion.

4.3. Simulation results under DC home daily load profile

The optimization algorithm has been tested assuming to supply a DC

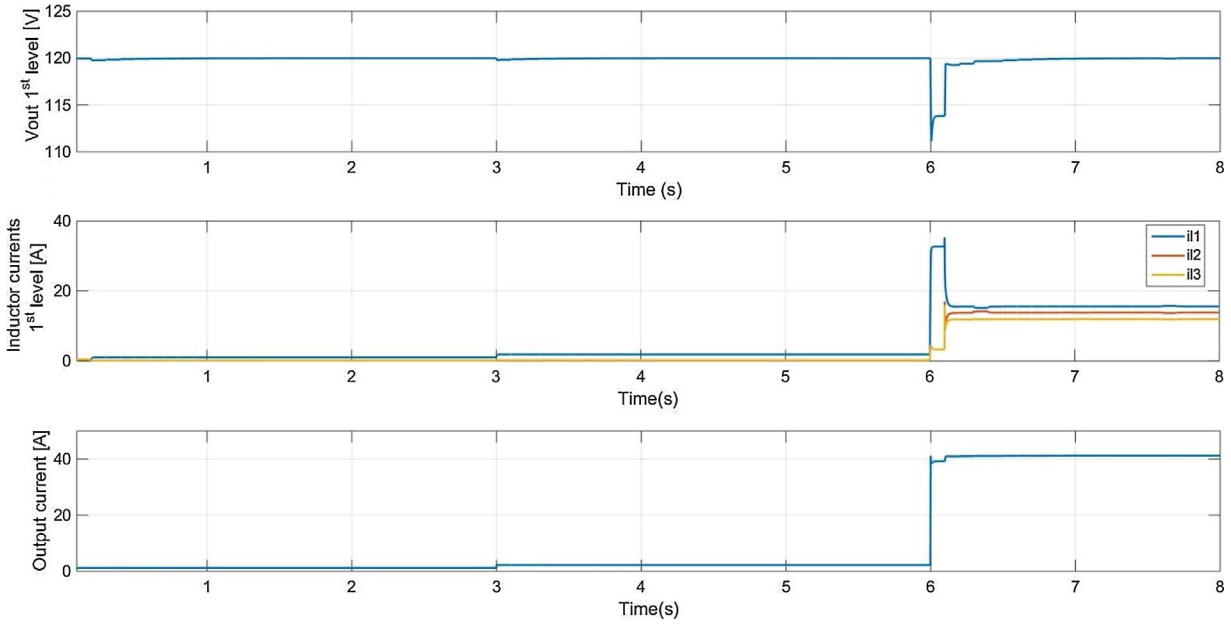

Fig. 7. Simulation results under load transients on the first level of conversion.

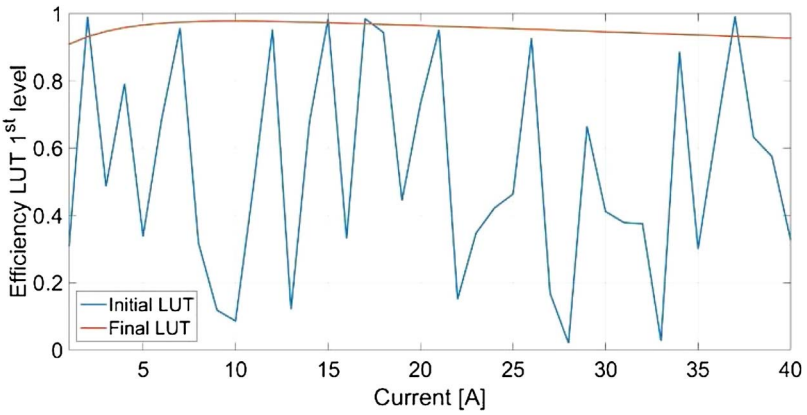

Fig. 8. Adaptive LUT process for a single converter in the first level of conversion.

home, whose load profile in a day has been evaluated by using the software developed by the University di Palermo and presented in (Graditi et al., 2015). Table 3 reports the loads considered in the study.

The load power profile of the second level of conversion and the corresponding current (whose values are readable by the second axis on the right) are shown in Fig. 12. The related input power profiles of the second level of conversion with and without GA are shown in Fig. 13. The profile without GA shows higher input power with respect to the case with GA, due to higher power losses.

Fig. 14 shows the efficiency gain at the second level of conversion due to the action of the GA. The maximum efficiency increase is about 3.8%.

The energy savings on the second level of conversion thanks to GA are equal to 37.14 Wh/day for a daily energy consumption of 1.16 kWh (3.2% of the total energy consumption). Assuming the same daily profile all year long, the yearly energy savings due to the action of the GA are equal to 13 kWh.

The total load profile of the first level of conversion, including the input power profile with or without GA on the second level, is shown in Fig. 15. Fig. 16 shows the input power profiles for the same level with and without GA on both conversion level.

As shown in Fig. 16, also in this case, GA action allows to minimize the energy losses, leading to a lower input power profile. The energy savings on the first level of conversion thanks to GA are equal to 394.13 Wh/day for a daily energy consumption of 7.4 kWh (5.3% of the total energy consumption). Assuming the same daily profile all year long, the yearly energy savings due to the action of the GA are equal to 144 kWh.

Fig. 17 shows the daily efficiency difference (with and without GA) under the daily load profile. The peak difference is equal to 5.74%.

4.4. Simulation results under DC home daily load profile with peak shaving

Finally, a Peak Shaving (PS) action is applied to the daily load profile of the first level of conversion. Thanks to the software presented in (Graditi et al., 2015), PS has been achieved by shifting in time the power profile of the dishwasher, the washing machine and the electric storage water heater.

Concerning the power conversion efficiency, benefits brought by the PS must be evaluated considering the efficiency curve. Fig. 18 shows the efficiency curves of the first level of conversion with and without GA. Considering the curve with GA, two regions can be identified:

- region A at the left of the peak efficiency value, corresponding to light load condition;
- region B at the right of the peak efficiency value, corresponding to heavy load condition.

Within region A, efficiency increases as load current increases, whereas within region B efficiency increases as load current decreases. Consequently, if the peak power of the load stays in region B, a PS action could increase or decrease the conversion efficiency of the system. For example, if the peak operating point in Fig. 18 is D, the PS action enhances the conversion efficiency if the shaved peak remains in the region between points D and E, which share the same value of conversion efficiency. On the contrary, if the PS action reduces the peak current to a value below that corresponding to point E, the PS strategy worsen the power system efficiency. If the system works around the peak power conversion efficiency, the PS strategy is not useful to enhance the power conversion efficiency.

A comparison could be performed on advantages brought by the PS with and without GA. Considering both efficiency curves, three regions are highlighted in Fig. 18:

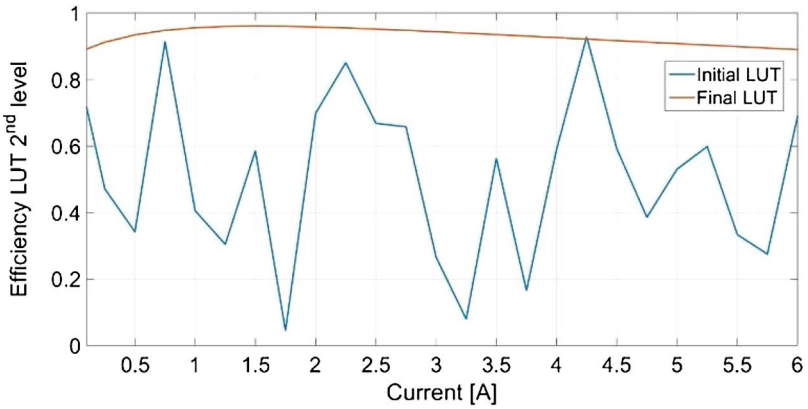

Fig. 9. Adaptive LUT learning process for a single converter in the second level of conversion.

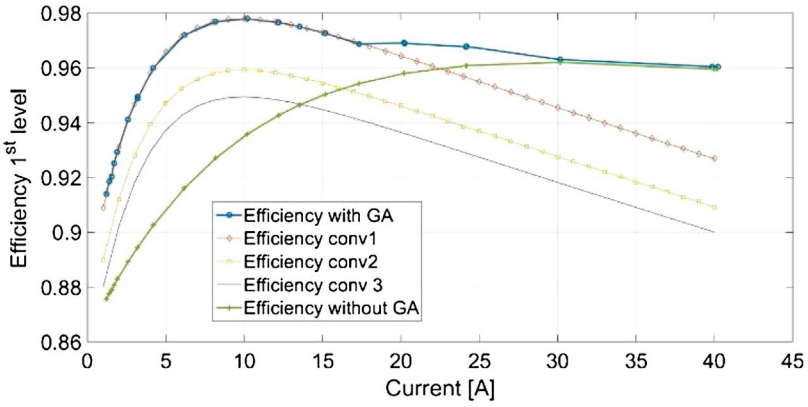

Fig. 10. Comparison of efficiency curves of each concurrent converter of the first level of conversion, efficiency curve of the whole level of conversion with and without GA.

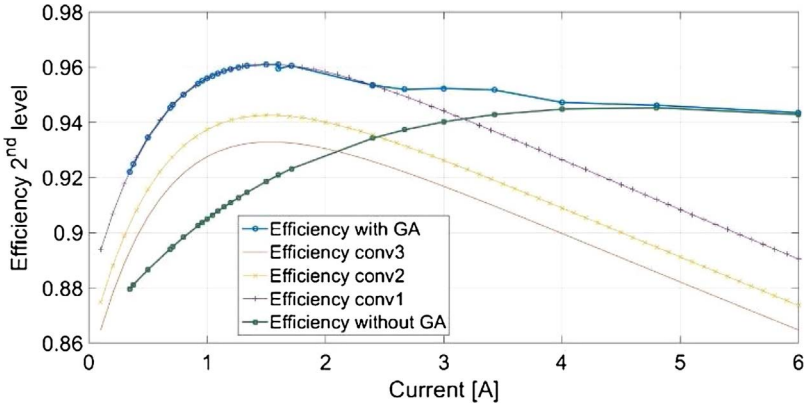

Fig. 11. Comparison of efficiency curves of each concurrent converter of the second level of conversion, efficiency curve of the whole level of conversion with and without GA.

Table 3
Characteristics of the appliances used in the simulation.

Appliance	Supply voltage level [V]	Maximum power [W]	Average time of use [minutes]
Entrance Lighting	24	10	20
Living Lighting	24	20	180
Kitchen Lighting	24	20	240
Corridor Lighting	24	8	10
Bathroom Lighting	24	12	60
Bedroom 1 Lighting	24	15	60
Bedroom 2 Lighting	24	15	30
Doorphone	24	40	1440
PC	120	70	120
HI-FI	120	60	30
TV + VHS + DVD	120	200	210
Hair-dryer	120	1000	20
Vacuum cleaner	120	2000	70
Microwave oven	120	600	15
Exhaust fan	120	100	30
Electric iron	120	2000	20
Washing machine	120	2000	90
Electric oven	120	1600	70
Fridge + Freezer	120	260	210

- region (a) where both curves increases with increasing current;
- region (b) where the GA efficiency curve decreases with increasing current and the efficiency curve without GA increases with increasing current;
- region (c) where the two efficiency curves nearly overlaps, decreasing with increasing current.

If the peak power relies in region (a), PS is not useful to enhance the power conversion efficiency but without GA the efficiency will be even worsened since the efficiency values are less than with enabled GA. If the peak relies in region (b) and the GA is enabled, PS enhances the efficiency if the shaved peak remains in region (b) or moves towards the region (a) up to the symmetric point to the red dashed line. On the contrary, if GA is disabled, a PS action always worsen the efficiency of the system. If the peak power relies in region (c), PS enhances the efficiency of the whole system equally with or without GA, provided that the shaved peak remains within region (c). If PS moves the peak towards region (b), efficiency with GA will be heavily enhanced. On the contrary, efficiency without GA will be slightly enhanced if the shaved peak remains in the region up to the symmetric point to the black dash-dotted line, otherwise the efficiency without GA will be heavily worsened. For example in Fig. 18, if the peak operating point is F, without GA the PS is useful in the region between F and G, symmetric points to the black dashed line sharing the same value of conversion efficiency. Even in this case, like in region (b), benefits brought by the PS with enabled GA over disabled GA are beyond argument.

After all, benefits brought by the PS should be evaluated by considering the efficiency curves. In some cases, the efficiency could be even worsened by applying the PS. It is worth to notice that peak efficiency and current regions are closely related to the specific power system under test, depending on load current, input voltage, switching frequency, components' ageing and components' loss parameters. If the power conversion efficiency is concerned, considerations on the chance of applying PS should be performed on the specific power system under test and actual working conditions.

In the present case study, both the peak power and the shaved peak power rely in region (b). Consequently PS is advantageous and the power conversion efficiency with PS benefits from GA. The peak power is reduced from 2.3 kW to 2 kW by shifting in time the activation of the washing machine and of the dishwasher. The total output power profile, including the second level input power profile with GA, is shown in Fig. 19.

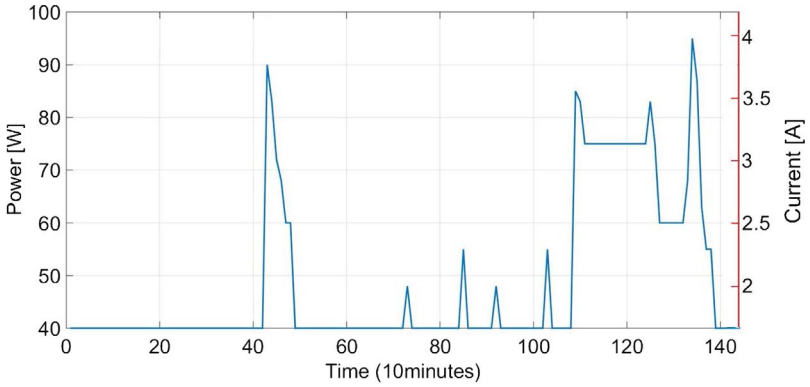

Fig. 12. Load power daily profile on the second level of conversion.

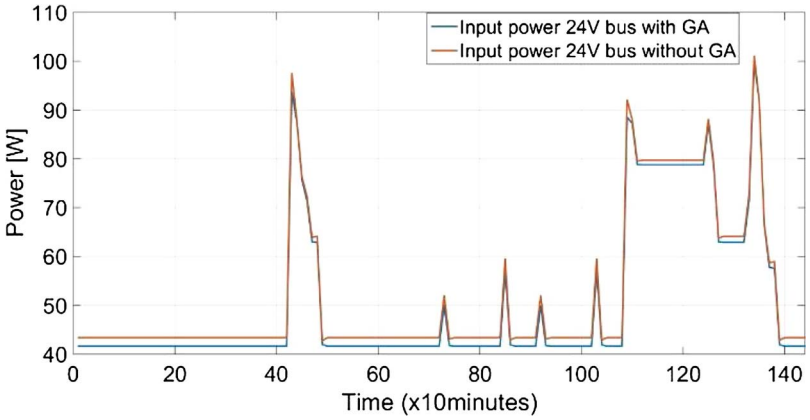

Fig. 13. Daily profile of the input power of the second conversion level with and without GA.

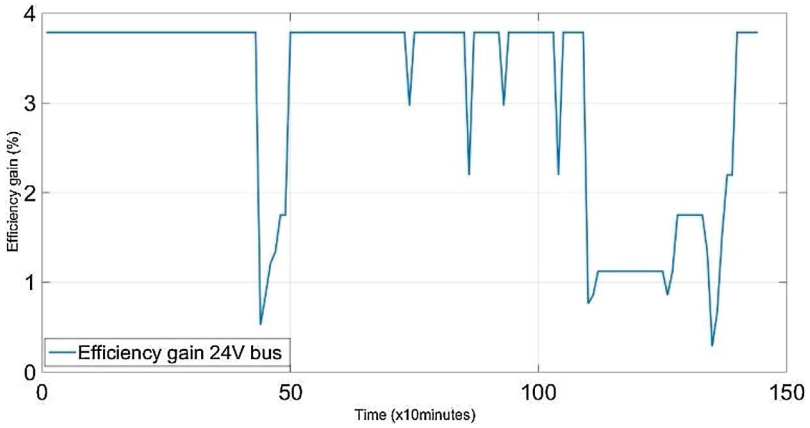

Fig. 14. Efficiency gain with GA at the second level of conversion.

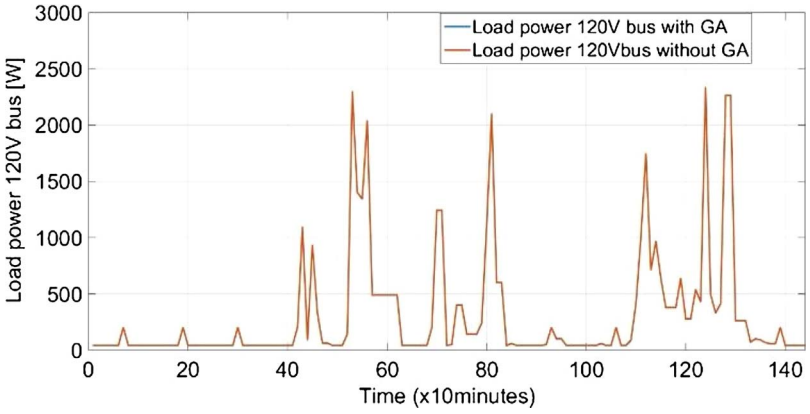

Fig. 15. Load power daily profile on the first level of conversion.

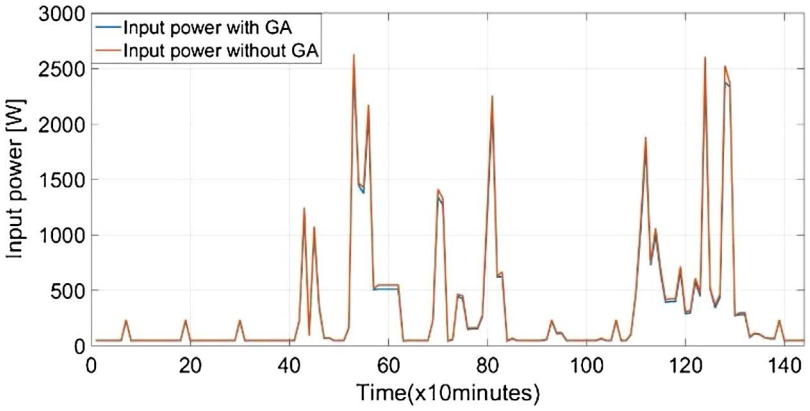

Fig. 16. Daily profile of the input power of the first conversion level with and without GA.

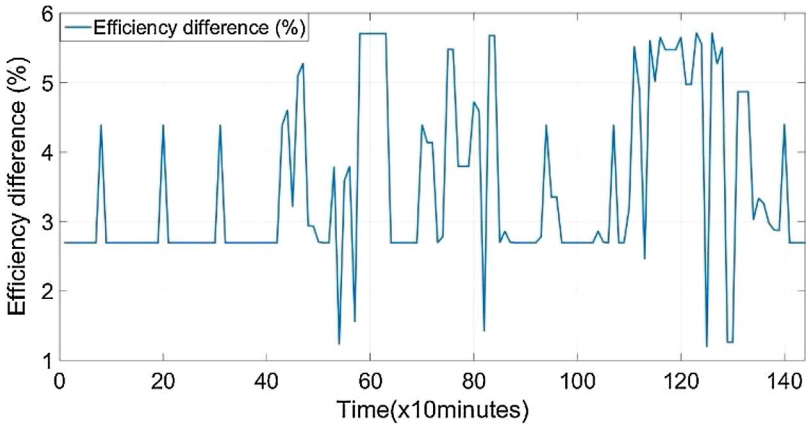

Fig. 17. Efficiency difference with and without GA under daily load profile.

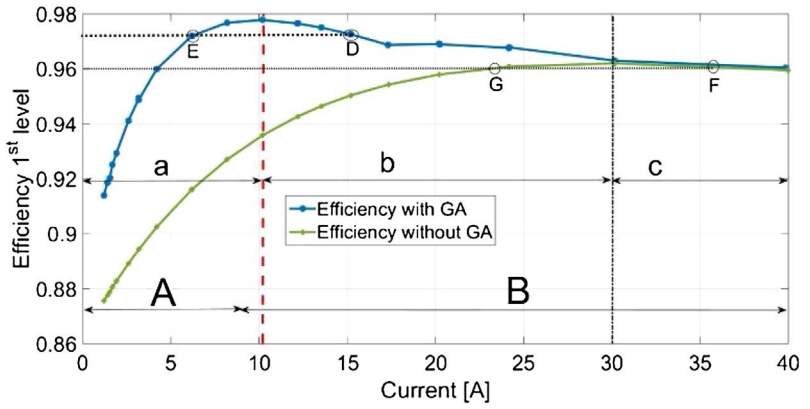

Fig. 18. Benefits brought by PS on the power conversion efficiency with and without GA.

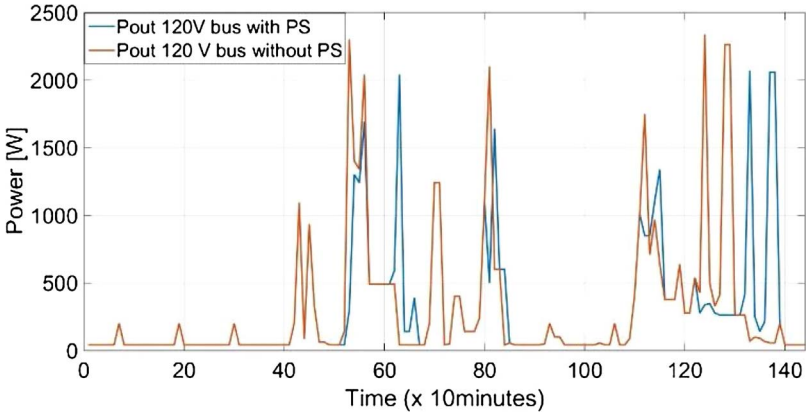

Fig. 19. Load power profile with and without PS.

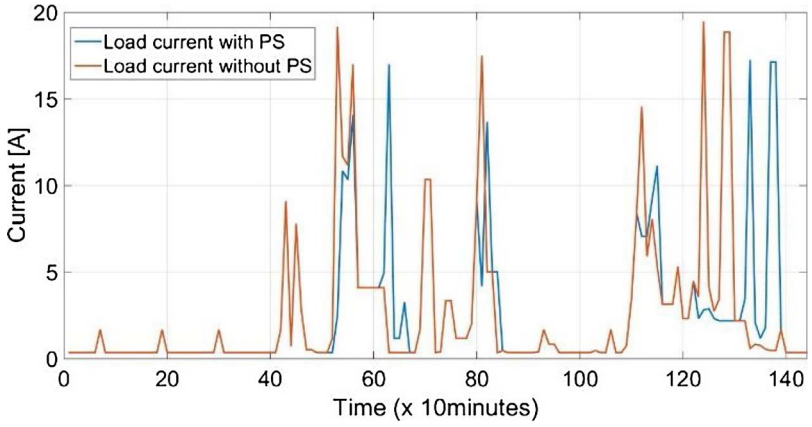

Fig. 20. Load current profile with and without PS.

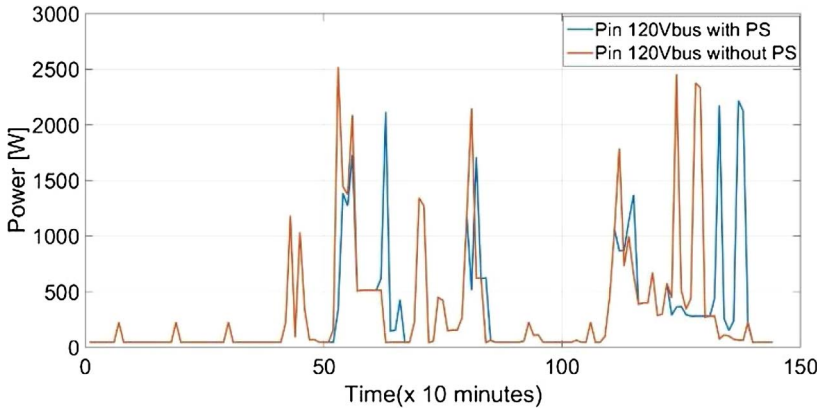

Fig. 21. Input power profile with and without PS.

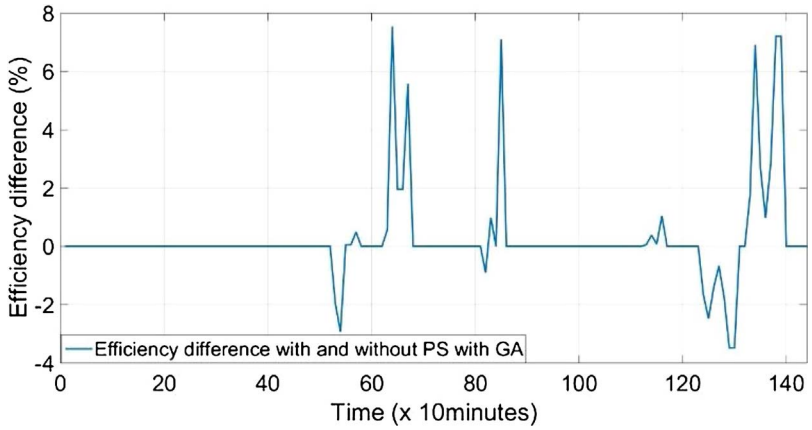

Fig. 22. Efficiency difference with and without PS.

The corresponding load current profile with and without peak shaving is shown in Fig. 20. By reducing the peak current values, the system moves towards higher efficiency values.

Fig. 21 shows the input power of the first level of conversion with and without PS. The difference between the input power with PS and without PS has been integrated over the whole day and it is equal to 20.13 Wh, corresponding to the 0.27% of the output daily energy consumption. Assuming the same daily profile all year long, the energy saving due to PS is equal to 7.3 kWh/year.

The efficiency difference with and without PS is shown in Fig. 22. The maximum efficiency difference is equal to 7.54% and the average value is equal to 0.27%.

5. Conclusions and future work

In this paper, an online efficiency optimization algorithm has been implemented in a LVDC microgrid supplying residential loads. The algorithm is based on a GA which generates the optimal current sharing ratios among concurrent converters in order to minimize losses of the whole power system. The use of heuristics instead of classical deterministic optimization has been preferred due to the highly non linear nature of the efficiency curves of the DC/DC converters. The online algorithm has been preferred to off-line algorithms because the efficiency depends on several variables among which the switching frequency, the load current, input voltage, components'ageing and components' loss parameters. Simulations have been carried out considering several case studies to validate the proposed solution. Benefits brought by GA have been widely discussed. Under a daily DC

home load profile, thanks to the implemented GA, power saving is equal to 143 kWh/year for a 7.4 kWh daily power. PS has been applied for evaluating possible concurrent benefits. Benefits brought by PS in terms of power conversion efficiency have been widely discussed with and without GA. In order to benefit from PS, efficiency curves of the power system under test for actual working conditions should be carefully analyzed. In the simulated case study, thanks to peak shaving, the power saving is increased by 7.3 kWh/year. By applying both GA and PS a total power saving of 150.3 kWh/year is obtained.

A few possible future developments are envisaged for this work. First of all the same approach will be tested using a Data Center load profile. In these cases, the load shows a large variation during the 24 h time frame and the benefit in terms of overall efficiency improvement is probably more evident. Secondarily, a hop mode technique will be implemented to further enhance the efficiency of the whole system under light load conditions. Under light load conditions, a variable switching frequency control will be applied, reducing the switching frequency as a function of the load current. The GA algorithm will be applied to a variable switching frequency control for light load conditions and a fixed frequency control for medium-heavy load current values. Thirdly, an interpolation of the efficiency curve could be used to express under closed form the entire optimization problem, so as to employ available deterministic NLP optimization tools.

References

Amin, M., Arafat, Y., Lundberg, S., & Mangold, S. (2011a). Low voltage DC distribution system compared with 230 V AC. In: *Proc. EPEC,* 340–345.

Amin, M., Arafat, Y., Lundberg, S., & Mangold, S. (2011b). An efficient appliance for low voltage DC house. In: *Proc. 2011 IEEE electrical power and energy conference,* 334–339.

Anonymous (2017). *Intelligent microgrid living lab.* [available at: http://www.et.aau.dk/research-programmes/microgrids/activities/intelligent-dc-microgrid-living-lab/].

Das, J. P., Fatema, R. J., & Anower, M. S. (2016). Feasibility study of low voltage DC distribution system for residential buildings in Bangladesh and hybrid home appliance design for tropical climate. In: *Proc. ICECTE,* 1–4.

Diaz, E. R., Su, X., Savaghebi, M., Quintero, J. C. V., Han, M., & Guerrero, J. M. (2015). Intelligent DC microgrid living laboratories - a Chinese-Danish project. In: *Proc. ICDCM,* 1–6.

Diaz, E. R., Vasquez Quintero, J. C., & Guerrero, J. M. (2016). Intelligent DC homes in future sustainable energy systems. *IEEE Consumer Electronics Magazine, 1*(January (5)), 74–80.

Dragičevíc, T., Lu, X., Vasquez, J. C., & Guerrero, J. M. (2016a). DC microgrids—part II: A review of power architectures, applications and standardization issues. *IEEE Transactions on Power Electronics, 31*(May (5)), 3528–3549.

Dragičevíc, T., Lu, X., Vasquez, J. C., & Guerrero, J. M. (2016b). DC microgrids—part I: A review of control strategies and stabilization techniques. *IEEE Transactions on Power Electronics, 27*(4), 4876–4891.

Dragicevic, T., Vasquez, J. C., Guerrero, J. M., & Skrlec, D. (2014). Advanced LVDC electrical power architectures and microgrids: A step toward a new generation of power distribution networks. *IEEE Electrification Magazine, 2*(March (1)), 54–65.

Garbesi, K., Vossos, V., & Shen, H. (2011). *Catalog of DC appliances and power systems.* Berkeley National Laboratory. available at: https://ees.lbl.gov/sites/all/files/catalog_of_dc_appliances_and_power_systems_lbnl-5364e.pdf.

Glasgo, B., Azevedoa, I. L., & Hendricksonb, C. (2016). How much electricity can we save by using direct current circuits in homes? Understanding the potential for electricity savings and assessing feasibility of a transition towards DC powered buildings. *Applied Energy, 180*, 66–75.

Goldberg, D. E. (1989). *Genetic algorithms in search, optimization and machine learning.* Addison Wesley.

Graditi, G., Ippolito, M. G., Lamedica, R., Piccolo, A., Ruvio, A., Santini, E., et al. (2015). Innovative control logics for a rational utilization of electric loads and air-conditioning systems in a residential building. *Energy and Buildings, 102*(September), 1–17.

Guerrero, J. M., Vasquez, J. C., Matas, J., de Vicuna, L. G., & Castilla, M. (2011). Hierarchical control of droop-controlled AC and DC Microgrids—a general approach toward standardization. *IEEE Transactions on Power Electronics, 58*(1), 158–172.

IEC Standard 60364-4-41 (2005). *IEC standard 60364-4-41:2005, low-voltage electrical installations − part 4-41: Protection for safety − protection against electric shoc*.

Justo, J. J., Mwasilu, F., Lee, J., & Jung, J. (2013). AC-microgrids versus DC-microgrids with distributed energy resources: A review. *Renewable and Sustainable Energy Reviews, 24*, 387–405.

Kakigano, H., Miura, Y., Ise, T., Momose, T., & Hayakawa, H. (2008). Fundamental characteristics of DC microgrid for residential houses with cogeneration system in each house. In: *Proc. IEEE PESGeneral meeting, 2008,* 1–8.

Kakigano, H., Miura, Y., Ise, T., Van Roy, J., & Driesen, J. (2012). Basic sensitivity analysis of conversion losses in a DC microgrid. In: *Proc. ICRERA,* 1–6.

Klimczak, P., & Munk-Nielsen, S. (2008). Comparative study on paralleled vs. scaled dc-dc converters in high voltage gain applications. In: *Proc. EPE-PEMC,* 108–113.

Lana, A., Nuutinen, P., Kaipia, T., Mattsson, A., Karppanen, J., Peltoniemi, P., et al. (2015). Prospects of development of LVDC electricity distribution system energy efficiency. *Proc CIRED,* 1–5.

Laudani, G. A., Mitcheson, P. D., Comparison of cost and efficiency of DC versus AC in office buildings, Repoert EP/I031707/1, Imperial College London, available at: http://www.topandtail.org.uk/publications/Report_ComparisonofCost.pdf.

Madduri, P. A., Poon, J., Rosa, J., Podolsky, M., Brewer, E., & Sanders, S. (2015). A scalable DC microgrid architecture for rural electrification in emerging regions. In: *Proc. APEC,* 703–708.

Makarabbi, G., Gavade, V., Panguloori, R., & Mishra, P. (2014). Compatibility and performance study of home appliances in a DC home distribution system. In: *Proc. PEDES,* 1–6.

Nasirian, V., Davoudi, A., & Lewis, F. L. (2014). Distributed adaptive droop control for DC microgrids. *Proc APEC, 1147*, 1152.

Nilsson, D., & Sannino, A. (2004). Efficiency analysis of low and medium- voltage DC distribution systems. *Proc IEEE PES general meeting,* 2315–2321.

Nuutinen, P., Kaipia, T., Peltoniemi, P., Lana, A., Pinomaa, A., Silventoinen, P., et al. (2014). Research site for low-voltage direct current distribution in utility network − structure, functions and operation. *IEEE Transactions on Smart Grid, 5*(September (5)), 2574–2582.

Rekola, J., & Tuusa, H. (2014). Efficiency of converters and amorphous core AC-filters in an LVDC distribution. In: *Proc. APEC,* 1827–1834.

Riva Sanseverino, E., Zizzo, G., Boscaino, V., Guerrero, J. M., & Meng, L. (2017). Active load sharing technique for on-line efficiency optimization in DC microgrids. In: *Proc. EEEIC,* 1–5.

Rodriguez-Diaz, E., Vasquez, J. C., & Guerrero, J. M. (2016). Intelligent DC homes in future sustainable energy systems: when efficiency and intelligence work together. *Transactions on Consumer Electronics Magazine, 5*(January (1)), 74–80.

Sasidharan, N., & Singh, J. G. (2017). A resilient DC community grid with real time ancillary services management. *Sustainable Cities and Society, 28*, 367–386.

Sasidharan, N., Madhu M, N., Singh, J. G., & Ongsakul, W. (2015). An approach for an efficient hybrid AC/DC solar powered Homegrid system based on the load characteristics of home appliances. *Energy and Buildings, 108*, 23–35.

Sasidharana, N., Madhu Ma, N., Govind Singha, J., & Ongsakul, W. (2015). Real time active power ancillary service using DC community grid with electric vehicles and demand response. *Procedia Technology, 21*, 41–48.

Vossos, V., Garbesi, K., & Shen, H. (2014). Energy savings from direct-DC in U.S. residential buildings. *Energy and Buildings, 69*(Part A), 223–231.

Weixing, L., Xiaoming Mo, M., Yuebin, Z., & Marnay, C. (2012a). On voltage standards for DC home microgrids energized by distributed sources. In: *Proc. IPEMC,* 2282–2286.

Weixing, L., Xiaoming Mo, M., Yuebin, Z., & Marnay, C. (2012b). On voltage standards for DC home microgrids energized by distributed sources. In: *Proc. IPEMC,* 2282–2286.

Wu, T. F., Chen, Y. K., Yu, G. R., & Chang, Y. C. (2011). Design and development of DC-distributed system with grid connection for residential applications. In: *Proc. ECCE Asia,* 235–241.

Yoza, A., Uchida, K., Yona, A., & Senjyu, T. (2012). Optimal operation of controllable loads in DC smart house with EV. In: *Proc. ICRERA,* 1–6.